Defluoridation of groundwater using diatomaceous earth: optimization of adsorption conditions, kinetics and leached metals risk assessment

Anthony A. Izuagie[a,*], Wilson M. Gitari[a], Jabulani R. Gumbo[b]

[a]Department of Ecology and Resource Management, University of Venda, Thohoyandou, South Africa, Tel. +27 717228420; email: aaizuagie@gmail.com (A.A. Izuagie), Tel. +27 765956869; email: mugera.gitari@univen.ac.za (W.M. Gitari)
[b]Department of Hydrology and Water Resources, University of Venda, Thohoyandou, South Africa, Tel. +27 825121805; email: jabulani.gumbo@univen.ac.za

ABSTRACT

In Sub-Saharan Africa, many rural communities depend on boreholes as the most appropriate source of water supply. Sadly, water from some of the boreholes contains fluoride above the WHO guideline of 1.5 mg/L. Hence, defluoridation is necessary. The aim of this study is to investigate the fluoride uptake capacity of diatomaceous earth (DE), a natural resource at optimized conditions by batch method. X-ray fluorescence analysis showed that the major component is silica (83.1%), while Al_2O_3 is the main minor component. XRD shows it is an amorphous material. For 8 mg/L fluoride spiked water, the highest per cent fluoride removal at optimum adsorption conditions (contact time: 30 min, adsorbent dosage: 8 g/L, pH 2, temperature: 298 K and shaking speed: 200 rpm) was between 23.4 and 25.6%. PO_4^{3-} in tested field water was observed to reduce the fluoride uptake capacity of fluoride. The sorption data fitted better into Freundlich isotherm than Langmuir isotherm. Fluoride sorption process was found to be a second-order kinetic. Inductively coupled plasma-mass spectrometer analysis of treated water revealed that metal and non-metal species were released at trace levels. Modification of DE would be necessary to enhance the fluoride adsorption capacity of DE.

Keywords: Defluoridation; Optimization; Kinetics; Leached metals; Assessment

1. Introduction

Groundwater is considered to be the most preferred drinking water for most rural communities in countries such as India, Tanzania, Kenya and South Africa. The reason is not farfetched. Groundwater is usually free from waterborne diseases associated with surface water. Although groundwater may be free of pathogens, the level of fluoride it contains is worthy of note as too low or too high concentration of fluoride in drinking water is detrimental to health.

Fluoride is important for healthy teeth at concentration of 0.5–1.0 mg/L in drinking water [1]. It is observed that absence or too low concentration (<0.5 mg/L) in drinking water could lead to dental caries in children where newly developed enamel wears away as a result of acid produced from action of bacteria on sugar [2]. A guideline of 1.5 mg/L for fluoride in drinking water was set WHO [3]. In South Africa, a guideline of 0.75 mg/L was set for fluoride in drinking water, putting into consideration the average daily air temperature and water consumption [4].

*Corresponding author.

It is reported that drinking water containing fluoride concentration above 1.5 mg/L cause dental and skeletal fluorosis; the severity depending on the concentration of fluoride in drinking water [5–7]. High doses of fluoride interfere with carbohydrate, lipid, protein, vitamin, enzyme and mineral metabolism [4]. There is also damage to soft tissues of the body like the kidney [8].

A number of studies revealed fluoride concentrations above the WHO guideline of 1.5 mg/L in some borehole water in South Africa and a few African countries [9–13]. In the absence of piped borne water, most rural community dwellers depend on the fluoride-rich groundwater as the most acceptable water for consumption. Knowing the hazard excess fluoride in drinking water causes to human health, it is important to remove excess fluoride to a level acceptable for human consumption.

There are different defluoridation techniques. However, defluoridation based on the principle of adsorption is considered to be the most suitable for rural households [9,14,15]. This is because the technique is cheaper and does not require electricity or skill to operate. Most point-of-use domestic defluoridation units are adsorption based. A typical unit is illustrated by Venkobachar et al. [16].

The major component of an adsorption based defluoridation technique is the adsorbent. A number of adsorbents–natural and modified have been investigated for their fluoride removal potential. Many natural and synthetic materials have been studied to evaluate their defluoridation potentials. These include activated alumina [17], natural and metal oxide-modified bentonite clay [18], activated coconut charcoal [19], surface-tailored zeolite [20], magnesia-amended activated alumina granules [21] and lanthanum hydroxide [22] and synthetic hydroxyapatite [23]. There certainly is no end to the study of likely materials for defluoridation.

It is desirable that a material serving as an adsorbent be locally sourced, abundant and cheap. These factors made diatomaceous earth (DE) a good candidate for investigation. DE is non-toxic and naturally abundant. A study showed that the structure of DE contains bonded hydroxyl groups which could be exchangeable with electronegative fluoride [24].

2. Materials and methods

2.1. Preparation of sample

The DE for the study was obtained from natural deposits at Kariandusi in Gilgil District, Nakuru County, Kenya. Some quantity of the material was washed in deionized water to remove dirt and silt. The colloidal particles were recovered from suspension through centrifugation. The cleaned DE was dried in the oven at 110°C for 8 h, cooled in the desiccator, later crushed in a mortar until the particles could pass through 250-μm test sieve and then stored in corked bottles to prevent moisture absorption.

2.2. Characterization of natural DE

2.2.1. Morphology by scanning electron microscope

The structure of DE at the surface was elucidated by scanning with Hitachi X-650 scanning electron micro analyser equipped with CDU lead detector at 25 kV. As shown in Fig. 1, each elongated or pinnate diatom contained a set of regular arrays of rectangular pores arranged along the void tubes.

2.2.2. Physicochemical analysis

The chemical composition of the natural DE samples were analysed using Thermo Fisher ARL Perform'X Sequential XRF with OXSAS software. The samples were milled in a tungsten-carbide milling pot to achieve particle sizes <75 μm. The samples were dried at 100°C and roasted at 1,000°C to determine Loss on Ignition (LOI) values. One gram sample was mixed with 6 g of lithium tetraborate flux and fused at 1,050°C to make a stable fused glass bead. For trace elements analyses, the sample was mixed with PVA binder and pressed in an aluminium cup at 10 tonnes.

The results of the major elements composition are reported in terms of the percentage oxide in Table 1. Results showed that silica (SiO_2) is the major composition of the DE, with Al_2O_3 being the main minor component. Metal-free DE has a molecular formula $SiO_2 \cdot nH_2O$.
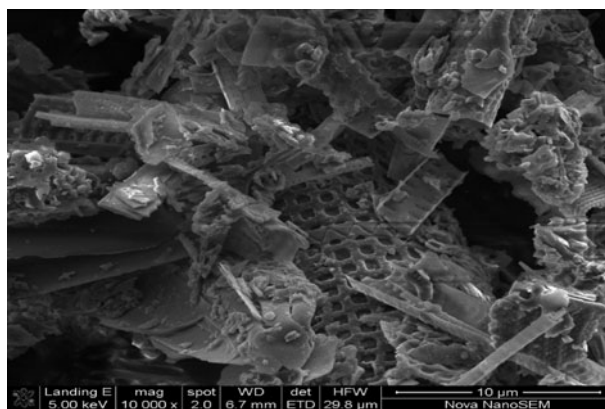

Fig. 1. SEM image of diatomaceous earth.

Table 1
Physicochemical parameters of DE

Oxide	Composition (%)
SiO_2	84.17
Al_2O_3	4.01
Fe_2O_3	2.96
Na_2O	0.61
K_2O	0.75
MgO	0.11
CaO	0.24
ZrO_2	0.06
TiO_2	0.17
MnO	0.04
P_2O_5	0.04
LOI[a]	7.52
pH_{pzc}[b]	(8.68)
WRC[c]	(2.25)

[a]Loss on ignition.
[b]pH at point-of-zero-charge.
[c]Water retention capacity (mL/g).

Table 2
Concentration of trace metals in DE

Trace element	Concentration (mg/kg)	Trace element	Concentration (mg/kg)
Sc	3.85	Pr	13.00
V	25.20	Nd	49.75
Cr	11.84	Sm	9.65
Co	1.43	Eu	0.90
Ni	7.38	Gd	8.42
Cu	17.55	Tb	1.48
Zn	86.93	Dy	9.41
Rb	44.67	Ho	2.05
Sr	26.74	Er	6.13
Y	51.45	Tm	0.91
Zr	453.15	Yb	6.24
Nb	85.41	Lu	0.89
Mo	2.36	Hf	11.32
Cs	1.20	Ta	5.04
Ba	30.97	Pb	11.08
La	58.50	Th	13.70
Ce	109.58	U	2.95

The water retention capacity (WRC) of DE was determined by dispersing 4 g of DE into 100 mL of deionized water, in a 250-mL bottle. The mixture was swirled for about 2 min and allowed to stand for 24 h after which the supernatant was decanted into a dry measuring cylinder. Nine millilitres of water was absorbed by DE. The WRC measured in millilitre per gram is reported in Table 1.

The pH at point-of-zero-charge (pH_{pzc}) of DE was determined using 1 M KCl. Aliquots of 40 mL of the KCl solution were measured into 250-mL plastic bottles followed by pH adjustment to selected values. The volume of solution in each bottle was made up to 50 mL by adding more KCl solution while noting the final pH on volume adjustment. A dosage of 1 g of DE was weighed into each bottle, corked and shaken at 250 rpm for 24 h. After equilibration, the equilibrium pH was quickly measured with a pH meter. The plot of change in pH against the initial pH gave a curve from which the pH_{pzc} was determined. The pH_{pzc} was the point on the curve for which change in pH was zero. This value was 8.68 as given in Table 1.

Full suite of trace elements in the DE sample was analysed by laser ablation inductively coupled plasma-mass spectrometer (ICP-MS) on fusion disc. The results are presented in Table 2. Zirconium had the largest concentration (453.15 mg/kg) followed by cerium (109.58 mg/kg).

2.2.3. X-ray diffraction analysis

The DE for the study was analysed for mineral composition using PANalytical X'Pert Pro powder diffractometer in θ–θ configuration with an X'Celerator detector and variable divergence- and fixed receiving slits with Fe filtered Co-Kα. The phases were identified using X'Pert Highscore plus software. The diffractogram of DE (Fig. 2) shows that the material is completely amorphous, containing no crystalline mineral phases.

2.2.4. BET analysis

The surface area, pore volume and pore width of DE of particle size <250 μm were evaluated using the Brunauer–Emmett–Teller (BET) method. The results of the measurements by Micromeritics TriStar II *Surface Area and porosity* are presented in Table 3.

2.2.5. FTIR spectroscopy

The Fourier transform infrared (FTIR) analysis of the raw DE and fluoride-loaded DE was carried out using Bruker: ALPHA FT-IR Spectrophotometer to identify the functional groups in the material. The transmittance at 453 cm^{-1} represents the Si–O–H stretching vibration, while the one at 1,055 cm^{-1} represents Si–O–Si stretching vibration. The overlap of the bands at 453 cm^{-1} and 1,055 cm^{-1} for the raw DE and fluoride-loaded DE is an evidence of low sorption of fluoride onto the DE surface. There was no significant change in the functional groups of the original material with fluoride sorption (Fig. 3).
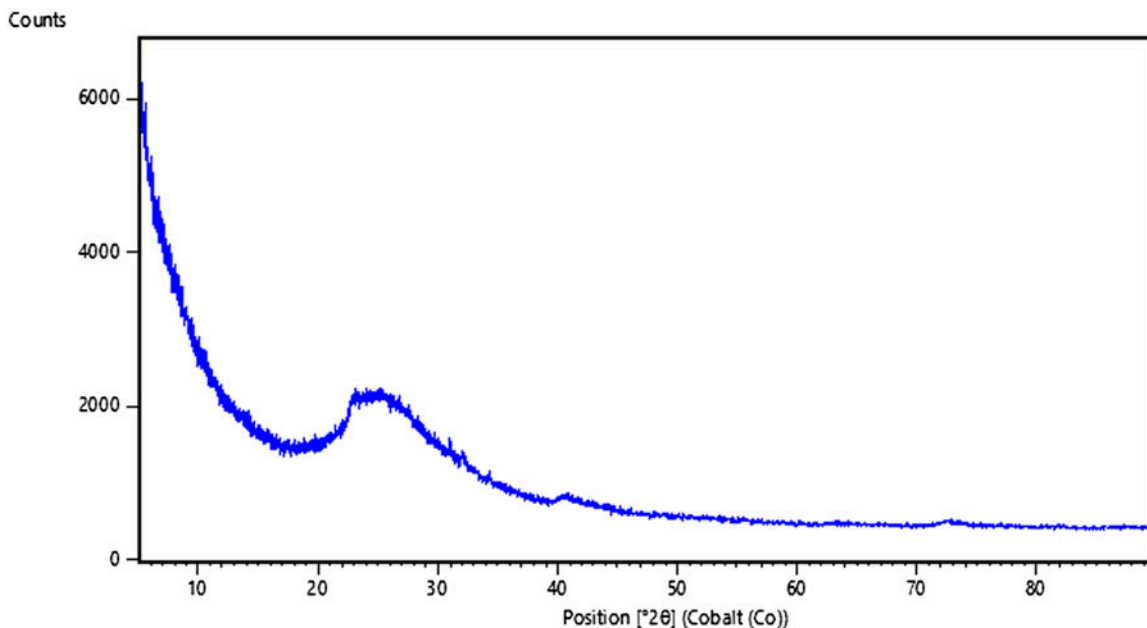
Fig. 2. X-ray diffractogram of raw DE.

Table 3
Surface dimensions of DE by BET

Parameter	Quantity		
	Area (m^2/g)	Volume (cm^3/g)	Pore (nm)
Single point surface area	31.1740		
BET surface area	31.8861		
Single point adsorption total volume		0.082691	
Adsorption average pore width (4 V/A by BET)			10.37335

2.3. Batch adsorption experiment

The adsorption of fluoride on DE was studied using batch adsorption equilibration method. Aliquots of 40 mL of fluoride solutions of known concentrations were first pipetted into 250-mL plastic bottles. Different masses of adsorbent were then weighed into the bottles followed by pH adjustment with 0.1 M HCl or 0.1 M NaOH, while noting the total volume of acid or/and alkali used. The final volume of solution was made up to 50 mL by adding deionized water. As a result of dilution a solution containing initially 10 mg/L fluoride had a final concentration of 8 mg/L. Bottles were corked and shaken in a reciprocating thermostated water bath shaker (Daihan LabTech Model LSB-015S). After equilibration, the suspensions were centrifuged at 5,000 rpm for 5 min. TISAB III was added to the supernatants at volume ratio of 1:10 to decomplex possible fluoride complex of aluminium or iron (III), prevent ionic strength variation and also

keep the pH between 5.2 and 5.5. The solutions were stirred and allowed to stand for 1 h for complete reaction. Fluoride in supernatants were determined using a fluoride ion-selective electrode (ORION VERSAS-TAR Advanced Electrochemistry meter fluoride ion-selective electrode) calibrated with four fluoride standards containing TISAB III at the volume ratio of 1:10 as in the case of the samples.

The per cent fluoride removal was calculated using Eq. (1):

$$\% \text{ fluoride removal} = \left(\frac{C_0 - C_e}{C_0}\right) \times 100 \qquad (1)$$

where C_0 (mg/L) and C_e (mg/L) are the initial and equilibrium fluoride concentrations respectively.

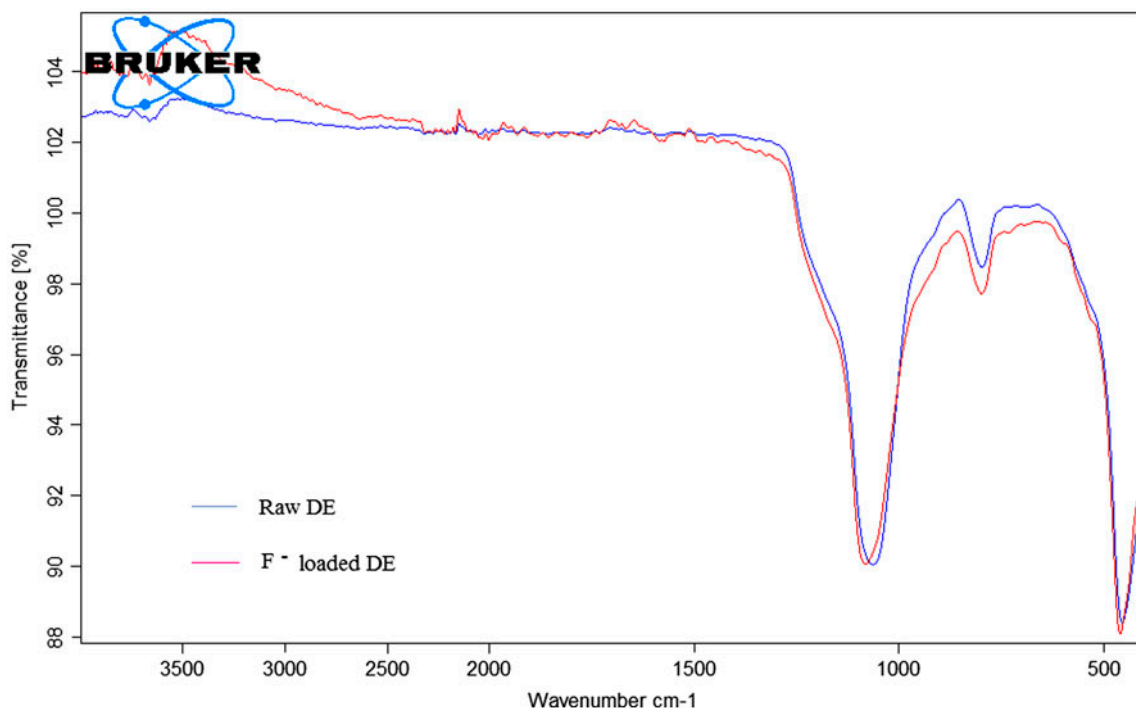The adsorption capacity (q_e) was calculated using Eq. (2):

Fig. 3. FTIR spectrum of raw and F⁻-loaded DE.

$$q_e = \frac{(C_0 - C_e)}{m} \times V \qquad (2)$$

where m (g) is the mass of adsorbent and V (L) is the volume of fluoride solution.

3. Results and discussions

3.1. Effect of shaking speed

The effect of shaking speed on fluoride sorption onto DE was evaluated at shaking speeds of 180, 200, 230 and 250 rpm. The equilibration of the mixtures consisting of 8 mg/L fluoride and adsorbent dosage of 0.4 g/50 mL were carried out at pH 2 and temperature of 298 K. After equilibration, the mixtures were centrifuged. The supernatants obtained were analysed for fluoride. Fig. 4 shows the trend in the per cent fluoride removal and the equilibrium pH as the shaking speed increased.

In Fig. 4, it can be seen that the per cent fluoride removal remained constant (25.62%) for all the evaluated shaking speeds. This implies that the fluoride removal was independent of increase in shaking speed above the minimum shaking speed evaluated. The equilibrium pH was observed to increase slightly from 2.09 at 180 rpm to a constant value of 2.13 at 230 rpm. As the shaking speed increased, the rate of collision between the fluoride and adsorbent would increase.
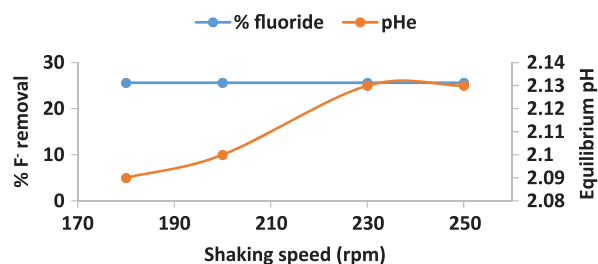

Fig. 4. Per cent fluoride removal as a function of shaking speed. Initial F⁻ concentration = 8 mg/L, volume of solution = 50 mL, adsorbent mass = 0.4 g, contact time = 30 min and temperature = 298 K.

Non-increase in the rate of fluoride sorption was probably due to increase in the equilibrium pH which would make the adsorbent surface less electropositive for fluoride attraction and removal from solution.

3.2. Effect of contact time

In consideration of the effect of contact time on fluoride sorption, mixtures of 8 mg/L fluoride and 0.4 g/50 mL sorbent dosage at pH were equilibrated for 5, 10, 20, 30, 40 and 50 min at 298 K and shaking speed of 200 rpm. After equilibration, the mixtures were centrifuged and the supernatants analysed for fluoride as explained in Subsection 2.3.
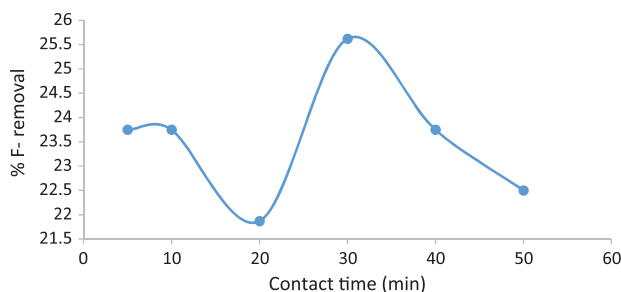
Fig. 5. Variation of per cent fluoride removal with contact time. Initial F⁻ concentration = 8 mg/L, volume of solution = 50 mL, adsorbent dosage = 0.4 g, temperature = 298 K, initial pH 2 and shaking speed = 200 rpm.
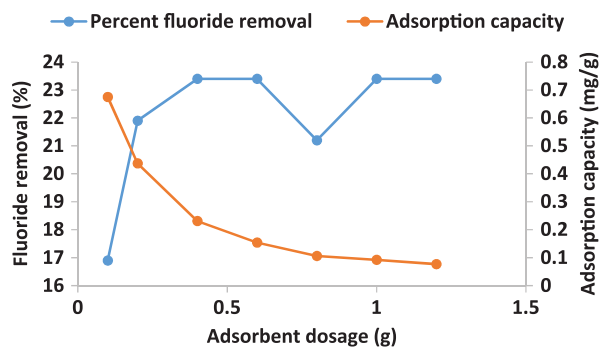

Fig. 6. Variation of a per cent fluoride removal and adsorption capacity with adsorbent dosage. Initial F⁻ concentration = 8 mg/L, volume of solution = 50 mL, contact time = 30 min, temperature = 298 K, initial pH 2 and shaking speed = 200 rpm.

The trend in the per cent fluoride removal at various contact times is presented in Fig. 5. At the start of defluoridation process, fluoride ions migrate to the adsorbent surface where they are adsorbed. As shaking continues some fluoride ions are desorbed from the surface while some are adsorbed. The adsorption-desorption process continues throughout the contact time. It can be seen that the rate at which adsorption and desorption occurred was the same for 5 and 10 min contact times. At 20 min contact time, fluoride desorption progressed faster than its adsorption, leading to a lower per cent fluoride removal from solution at this time. The amount of fluoride adsorption increased to the highest value of 25.62% at 30 min contact time. Above this time, fluoride desorption predominated over its adsorption. Hence, the optimum contact time was 30 min.

3.3. Effect of adsorbent dosage

The effect of adsorbent dosage on fluoride sorption onto DE was evaluated with the view of obtaining the optimum sorbent dosage. Sorbent dosage was varied from 0.1 to 1.2 g/50 mL. The initial concentration of fluoride solution was 8 mg/L while the initial pH of the sorbent–fluoride mixture was 2. The mixtures were equilibrated for 30 min at 200 rpm. After equilibration, the mixtures were centrifuged to remove the solid. The supernatants obtained were analysed for residual fluoride as explained previously.

The trend in the per cent fluoride removal and adsorption capacity at different adsorbent dosages are presented in Fig. 6. It was observed that the per cent fluoride removal increased from adsorbent dosage of 0.1 to 0.4 g/50 mL where the optimum per cent fluoride removal of 23.4% occurred. The increase in per cent fluoride removal was due to increase in the \number of adsorption sites as the dosage increased. The per cent fluoride removal at adsorbent dosage of

0.6 g/50 mL was the same as that of 0.4 g/50 mL. The increase in dosage must have resulted in overlapping of some active adsorption sites such that the net number of active adsorption sites equalled that obtained at 0.4 g dosage. At 0.8 g/50 mL dosage, more active sites overlapped, thereby reducing the number of net adsorption sites and the net surface area. Hence, there was a reduction of per cent fluoride removal. This observation is in conformity with reports from previous studies [25,26]. The per cent fluoride removal increased to a constant, optimum value of 23.4% at dosages of 1.0 g/50 mL and 1.2 g/50 mL. There was no observable increase in the per cent fluoride removal at these dosages because the number of overlapping sites was probably equal to the number of active sites. The optimum adsorbent dosage was therefore 0.4 g/50 mL.

The adsorption capacity decreased all through with increasing adsorbent dosage. This was notably because there was no appreciable increase in fluoride removal with increasing adsorbent dosage.

3.4. Effect of pH

To evaluate the effect of pH on fluoride sorption onto DE, mixtures consisting of 0.4 g/50 mL of adsorbent and 8 mg/L fluoride at pH 2–12 were equilibrated for 30 min at 200 rpm and 298 K. After equilibration, the sorbent was removed from the mixture by centrifuging, followed by analysis of the supernatants for residual fluoride.

The plots of the per cent fluoride removal against the corresponding equilibrium pH for the determinations are presented in Fig. 7. The positive values of per cent fluoride removal at equilibrium pH 2.05 and 4.27 are indicative of fluoride removal from solution at those pH values. The lower the
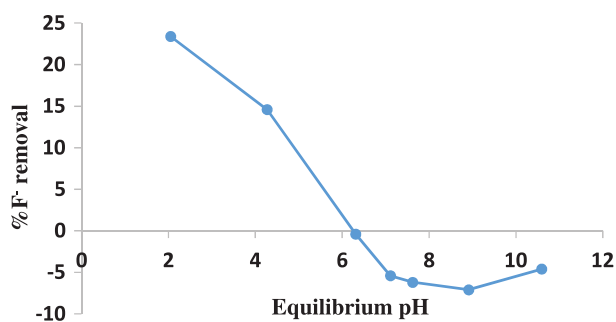
Fig. 7. Variation of per cent fluoride removal with equilibrium pH. Initial F^- concentration = 8 mg/L, volume of solution = 50 mL, contact time = 30 min, temperature = 298 K and shaking speed = 200 rpm.

pH, the higher the amount of fluoride removed. This must be due to the increase in the electropositivity of the adsorbent surface which enhanced attraction for the negatively charged fluoride. Above pH 6, negative values were obtained for per cent fluoride removal. Thus, fluoride was being leached from the sorbent rather than being removed from solution. The fluoride release is evidence that the DE contained geological fluoride. Generally, fluoride removal decreased with increasing pH. The optimum pH for fluoride removal from solution was at the lowest equilibrium pH of 2.05.

The chemistry of the fluoride removal at different pH may be explained in relation to the pH at point-of-zero-charge (pH_{pzc}) of the material. At pH_{pzc}, that is, 8.68, the surface charge of DE in solution was neutral. The surface of particles at pH less than the pH_{pzc} is positively charged [27]. Fluoride removal at the adsorbent surface therefore at $pH < pH_{pzc}$ was expected to be by electrostatic attraction of the fluoride ions by the positively charged surface. The more electropositive the surface was, the more the attraction for fluoride. This explains why the maximum fluoride removal (23.4%) occurred at pH 2.05 as shown in the profile in Fig. 7. Protonation of the silanols at the adsorbent surface provides sites for electrostatic attraction for fluoride. This occurs at acidic pH. Therefore, defluoridation at acidic pH would occur according to Eq. (4).

$$\equiv SiOH + H^+ \rightarrow \ \equiv SiOH_2^+ \tag{3}$$

$$\equiv SiOH_2^+ + F^- \rightarrow \ \equiv SiOH_2F \tag{4}$$
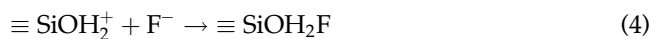
Precipitation of fluorides of iron and aluminium could contribute to fluoride removal at suitable pH as represented generally by Eq. (5):

$$M^{n+} + nF^- \rightarrow MF_n \tag{5}$$

where M is the metal and n+ is the charge of the metal ion.

The release of fluoride into solution arising from the geological fluoride component of DE could have resulted according to the reaction described in Eq. (6).

$$\equiv SiOH_2F + OH^- \rightarrow \ \equiv SiOH_2(OH) + F^- \tag{6}$$

3.5. Effect of adsorbate concentration

A number of studies have shown that within a certain range of adsorbate concentration, the amount of adsorbate removed from solution increases with adsorbate concentration [28–31]. Defluoridation was therefore carried out at varied initial fluoride concentrations to evaluate the effect of fluoride concentration on fluoride sorption onto DE. Mixtures of fluoride solution (8, 16, 24, 32, 40, 48, 64, 80 and 100 mg/L) and adsorbent (0.4 g/50 mL) at pH 2 were equilibrated for 30 min at 200 rpm. After equilibration, the mixtures were centrifuged and the supernatants analysed for residual fluoride.

Fig. 8 shows how the adsorption capacity and the per cent fluoride removal varied with the equilibrium fluoride concentration. The adsorption capacity was observed to increase with the equilibrium concentration. The steepness observed in the adsorption capacity profile decreased as from equilibrium fluoride concentration of 38.67 to 53.67 mg/L because the adsorbent surface was getting close to being completely covered by fluoride ions. This is evident from the drop of the per cent fluoride removal at the equilibrium fluoride concentration of 53.67 mg/L. With the
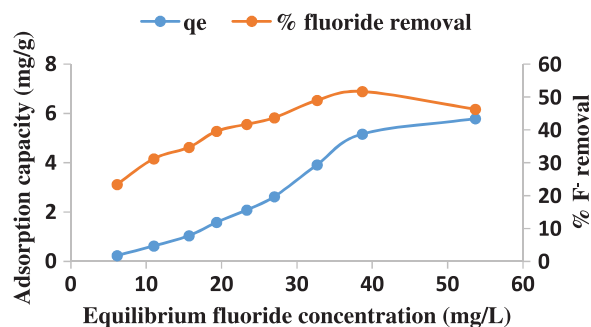

Fig. 8. Variation of adsorption capacity and per cent fluoride removal with equilibrium fluoride concentration. Volume of F^- solution = 50 mL, contact time = 30 min, initial pH 2, adsorbent dosage = 0.4 g and shaking speed = 200 rpm.

use of initial 100 mg/L fluoride solution, the surface of adsorbent was almost saturated with adsorbed fluoride at equilibrium. For the evaluated fluoride concentrations, the optimum fluoride removal occurred with defluoridation of solution containing initially 80 mg/L fluoride, while the optimum adsorption capacity was 5.7912 mg/g for the solution containing initially 100 mg/L fluoride solution. However, for this study, defluoridation of solution containing 8 mg/L fluoride was emphasized because the average fluoride concentration of the groundwater in the province of study was less than 8 mg/L.

3.6. Effect of temperature

The effect of temperature on fluoride sorption was evaluated by repeating the experiment described in subsection 3.5 at temperatures 313 and 323 K, respectively. Fig. 9(a) and (b) gives the comparison of the percentage fluoride removals and the adsorption capacities at different initial fluoride concentrations and evaluated temperatures respectively. It was observed that temperature variation did not have a significant effect on the amount of fluoride removed. Hence, defluoridation with DE could be done at ambient temperature at minimal energy expenditure.
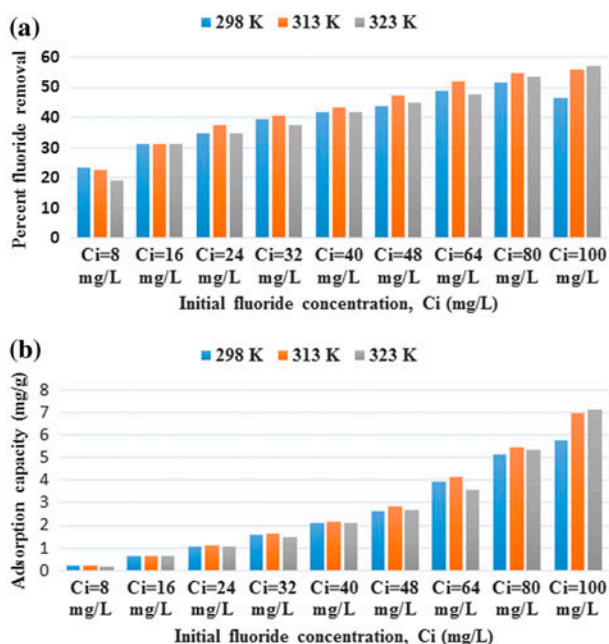

Fig. 9. Variation of (a) per cent fluoride removal and (b) adsorption capacity with temperature. Volume of F⁻ solution = 50 mL, contact time = 30 min, initial pH 2, adsorbent dosage = 0.4 g and shaking speed = 200 rpm.

3.7. Adsorption isotherms

The sorption data were modelled using Langmuir and Freundlich isotherms. Langmuir isotherm is used to test whether there was a monolayer adsorption of an adsorbate onto a smooth surface or not. The isotherm if applicable assumes that the surface containing the adsorbing sites is a perfectly flat (smooth) plane. Langmuir isotherm is given as:

$$q_e = \frac{q_m K_L C_e}{1 + K_L C_e} \tag{7}$$

where q_e is the adsorption capacity (mg/g), q_m is q_e for a complete monolayer (mg/g), C_e is the equilibrium concentration (mg/L) and K_L is the adsorption equilibrium constant (L/mg).

Linearized Langmuir equation known as Langmuir-1 is the most commonly used of the linear forms [32]. It is presented as:

$$\frac{C_e}{q_e} = \frac{1}{q_m} C_e + \frac{1}{K_L q_m} \tag{8}$$

The plot of C_e/q_e values against C_e gives a straight line with a positive slope $1/q_m$ if the adsorption data conform to Langmuir isotherm. No straight lines were however obtained when the Langmuir plots were done at the evaluated temperatures.

The sorption data were also modelled using Freundlich isotherm [33]. Freundlich isotherm describes a multi-site adsorption isotherm for rough surfaces.

Freundlich isotherm is given as:

$$q_e = K_F C_e^{1/n} \tag{9}$$

The linear form is:

$$\log q_e = \log K_F + \frac{1}{n} \log C_e \tag{10}$$

K_F and n are Freundlich constants whose values depend on experimental conditions. K_F represents the adsorption capacity while $1/n$ is the heterogeneity factor. $1/n$ values much less than 1 show that adsorbents are heterogeneous. K_F and $1/n$ can be obtained from the plots of $\log q_e$ against $\log C_e$. A linear plot means that the adsorption process conforms to the Freundlich isotherm. Values of $1/n$ close to 1 indicate a material with relatively homogeneous binding [34].
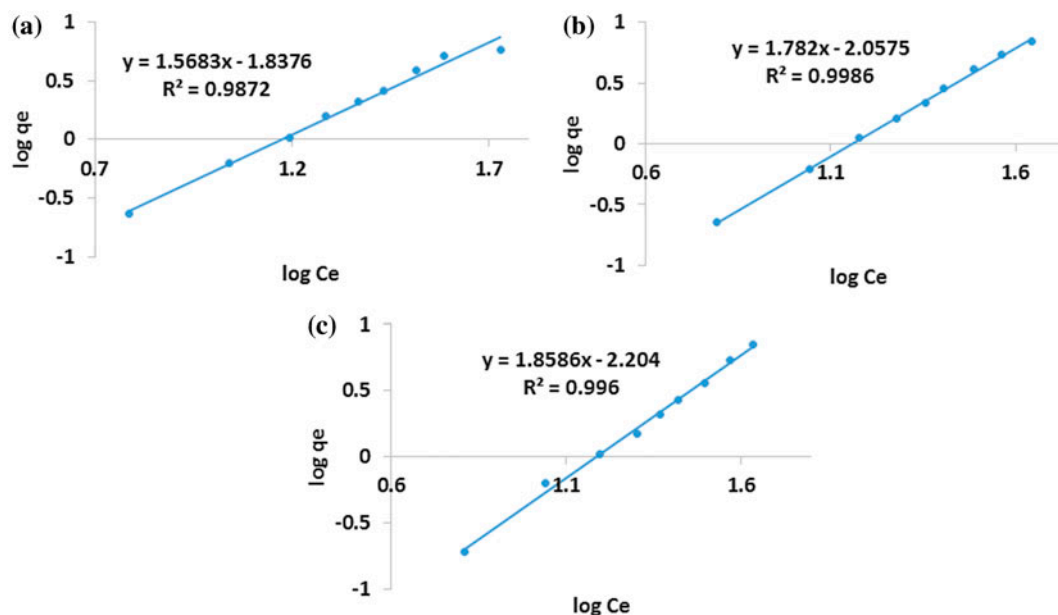
Fig. 10. Freundlich's profiles at (a) 298 K, (b) 313 K and (c) 323 K. Volume of F⁻ solution = 50 mL, contact time = 30 min, initial pH 2, adsorbent dosage = 0.4 g and shaking speed = 200 rpm.

Fitting of adsorption data into Freundlich isotherm at the evaluated temperatures gave plots with high linearity as shown in Fig. 10. It is therefore evident from the result that the fluoride adsorption onto raw DE is a multi-site adsorption. The low values of $1/n$ as shown in Table 3 are indicative of the heterogeneity of the surface of DE (Table 4).

3.8. Adsorption kinetics

The aims of studying chemical kinetics to include (1) to determine experimentally the rate of chemical reaction and its dependence on parameters such as concentration and temperature and (2) to understand the reaction mechanism, that is, the number of steps involved and the nature of intermediates formed. In the light of these facts, the kinetics of fluoride sorption onto DE was tested along the rate of chemical reaction and the likely mechanism controlling the sorption rate [35].

A number of mechanisms control a sorption rate. These include (1) diffusion from the bulk solution to a film layer surrounding the adsorbent particle, (2) diffusion from the film to particle surface, "film diffusion", (3) migration inside the adsorbent particle by "surface diffusion" or diffusion within liquid-filled pores, "pore diffusion" and (4) uptake of adsorbate by chemisorption, physicosorption, ion exchange or complexation [36,37].

The models for determining sorption mechanisms have been classified into two types. These are reaction-based and diffusion-based models [23].

3.8.1. Reaction-based models

The sorption data obtained from the equilibration of mixtures of 0.4 g of adsorbent and 50 mL of 8 mg/L fluoride solutions with initial pH 2 for 5, 10, 20, 30, 40 and 50 min at 298 K and shaking speed of 200 rpm were used.

The order for the sorption process was tested by fitting the sorption data into the Lagergren pseudo-first-order model [38] given as:

$$\frac{\mathrm{d}q_t}{\mathrm{d}t} = k_1(q_e - q_t) \tag{11}$$

q_t (mg/g) is the fluoride concentration at any time t, q_e (mg/g) is the maximum sorption capacity of the pseudo-first-order and k_1 (min⁻¹) is the pseudo-first-order rate constant.

Table 4
Calculated Freundlich isotherm parameters

Temperature (K)	K_F (mg/g)	$1/n$	R^2
298	0.0145	0.6376	0.9872
313	0.0088	0.5612	0.9986
323	0.0063	0.5380	0.9960

On integration, Eq. (11) becomes:

$$\ln(q_e - q_t) = -k_1 t + \ln q_1 \tag{12}$$

The plots of $\ln(q_e - q_t)$ values against t give a straight line with a negative slope for an adsorption that is a pseudo-first-order kinetic. However, the pseudo-first-order plots gave a scatter with a positive slope (figure not included).

Pseudo-second-order model was also applied to the data to determine its suitability in determining the order of the sorption process. The model is given as:

$$\frac{dq_t}{dt} = k_2(q_e - q_t)^2 \tag{13}$$

where q_t (mg/g) is the fluoride concentration at any time t, q_e (mg/g) is the maximum sorption capacity of the pseudo-second-order model and k_2 (g/(mg min)) is the rate constant for the pseudo-first-order process.

Integration of Eq. (13) gives the linear form of the pseudo-second-order model:

$$\frac{t}{q_t} = \frac{1}{k_2 q_e^2} + \frac{t}{q_e} \tag{14}$$

$$\frac{t}{q_t} = \frac{1}{h} + \frac{t}{q_e} \tag{15}$$

h (mg/(g min)) is the initial sorption rate defined as:

$$h = k_2 q_e^2 \tag{16}$$

The plots of t/q_t values against time t gave a straight line ($R^2 = 0.992$) as shown in Fig. 11. The closeness of the calculated q_e (0.2302 mg/g) to the experimental q_e
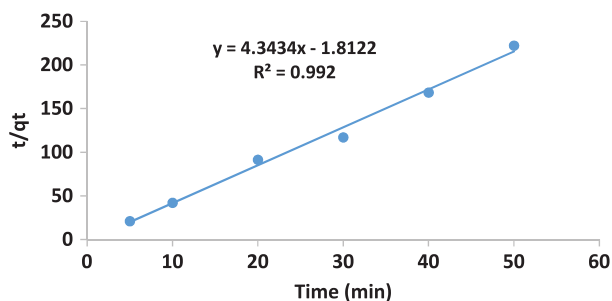
Fig. 11. Pseudo-second-order plots for defluoridation at different contact times. Initial F⁻ concentration = 8 mg/L, volume of solution = 50 mL, adsorbent dosage = 0.4 g, initial pH 2, temperature = 298 K and shaking speed = 200 rpm.

(0.2562 mg/g) is an indication that fluoride sorption onto DE is a second-order process. As a result, fluoride is chemisorbed onto DE as opposed to physisorption which is characterized by weak van der Waals forces.

3.8.2. Mechanism-based models

The possibility of intra-particle diffusion being the mechanism controlling the rate of adsorption of fluoride on DE was evaluated using the Weber–Morris model [39] stated as:

$$q_t = k_{id}\sqrt{t} + I \tag{17}$$

where k_{id} is the intra-particle diffusion rate constant (mg/(g min$^{1/2}$)) and I (mg/g) is a constant that has to do with the thickness of the boundary layer.

If the plot of q_t against $\sqrt{t}$ is linear, then, the sorption process would be controlled only by intra-particle diffusion. However, the plots gave a sinusoidal curve, showing that the sorption rate was not likely controlled by intra-particle diffusion.

The likelihood of external diffusion being the rate-controlling step was also tested using the model by Lee et al. [40]. The diffusion model is given as:

$$\ln\frac{C_t}{C_0} = -k_f \frac{A}{V} t \tag{18}$$

where C_0 is the initial fluoride concentration, C_t is the concentration at time t, A/V is the external adsorption area to the total solution volume, t is the adsorption time and k_f is the external diffusion coefficient. If a straight line is obtained from the plot of $\ln\frac{C_t}{C_0}$ against t, then, external diffusion controls the sorption process. The plot of $\ln\frac{C_t}{C_0}$ against t for the first 30 min of sorption gave a straight line (Fig. 12(a)) as described by Khraisheh et al. [41]. The linear plot obtained for the entire equilibration times (Fig. 12(b)) is an evidence that external diffusion was the rate-controlling mechanism for the sorption process.

3.9. Evaluation of metals, non-metals and anions release from DE

The safety of the DE for use in defluoridation of drinking water was evaluated by determining the extent of metals and non-metals released from the adsorbent into treated water at different equilibrium pH and contact times. The supernatants from the shaking of mixtures of 0.4 g of DE and 50 mL of 8 mg/L fluoride at different initial pH and contact
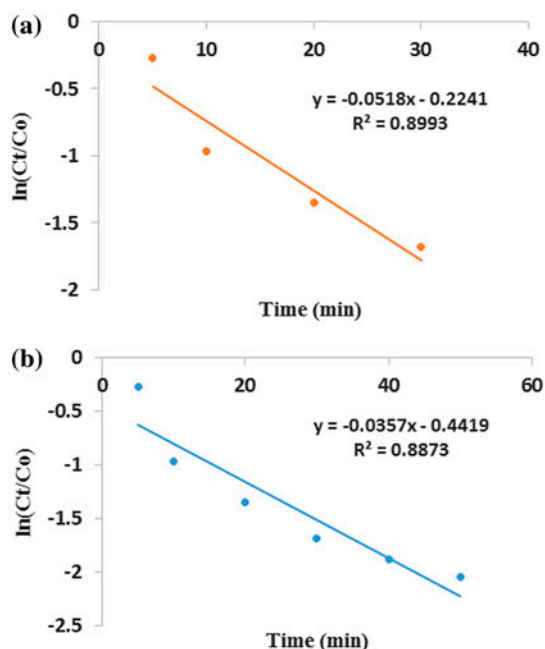
Fig. 12. External diffusion plots (a) for contact time up to 30 min and (b) for all contact time. Initial F^- concentration = 8 mg/L, volume of solution = 50 mL, adsorbent dosage = 0.4 g, initial pH 2, temperature = 298 K and shaking speed = 200 rpm.

Fig. 13. Concentration of metal and non-metal species in treated water at various contact times: (a) in mg/L and (b) in μg/L. Initial F^- concentration = 8 mg/L, volume of solution = 50 mL, adsorbent dosage = 0.4 g, initial pH 2, temperature = 298 K and shaking speed = 200 rpm.

Fig. 14. Concentration of elements in treated water at various equilibrium pH: (a) in mg/L and (b) in μg/L. Initial F^- concentration = 8 mg/L, volume of solution = 50 mL, adsorbent dosage = 0.4 g, initial pH 2, temperature = 298 K and shaking speed = 200 rpm.

times at 298 K and 200 rpm were analysed for major and trace elements using ICP-MS.

It was observed that all the metal and non-metal species released from the adsorbent into treated water were at trace levels and so the use of the DE for defluoridation might not portend danger as far as metal and non-metal release is concerned. The concentration of each species released into water was virtually independent of contact time (Fig. 13(a) and (b)). The amount of each metal species in water was a function of pH (Fig. 14(a) and (b)). The high concentrations of sodium observed were due to the NaOH used for necessary pH adjustment. The concentration of silicon in water was appreciably high at high equilibrium pH. This was so because of the increase in dissolution of silica at high equilibrium pH. The lowest silica dissolution was at the equilibrium pH 2.05.

Anions in treated water were analysed using Ion Chromatography on a Waters 432 Conductivity detector, coupled to a Waters 717plus Auto sampler and an Agilent 1,100 series binary pump. Anions evaluated included Cl^-, Br^-, SO_4^{2-}, PO_4^{3-}, NO_2^- and NO_3^-. Except for Cl^- whose average concentration was 391.26 mg/L in the supernatants because HCl was used to achieve an initial pH 2, none of the anions was detectable by the instrument at detection limit of 1 mg/L. The DE is
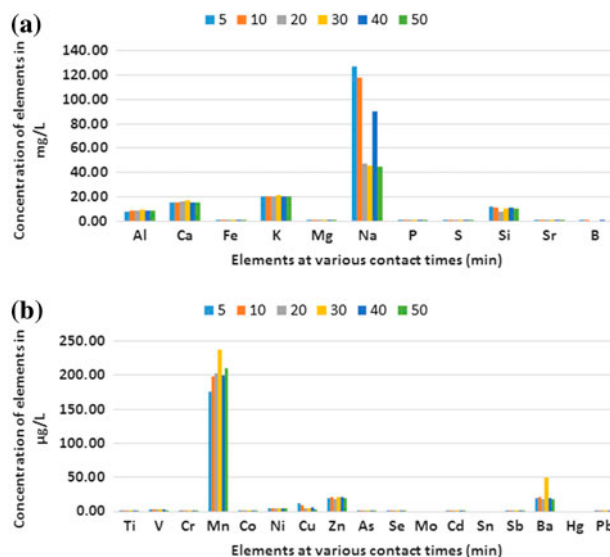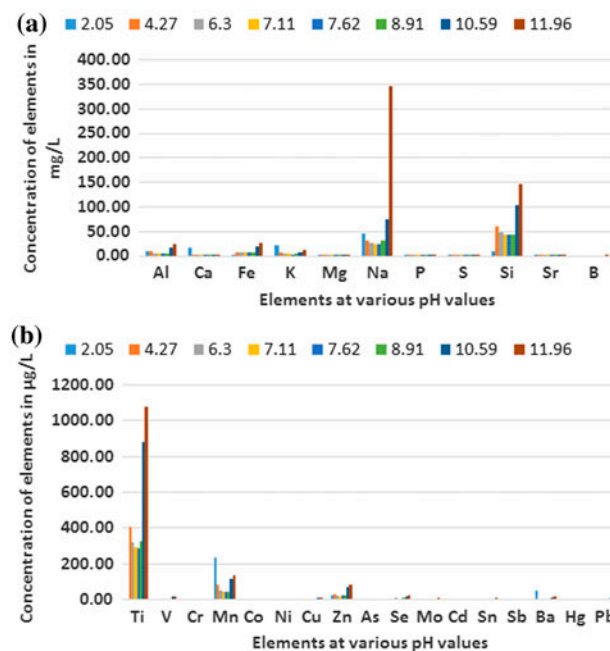
therefore safe for use in defluoridation of drinking water.

Table 5
Concentrations of anions in raw and treated field water

Anion	Anion concentration in raw field water (mg/L)	Anion concentration in treated field water (mg/L)
F^-	4.8	4.1
NO_3^-	ND	ND
PO_4^{3-}	2.4	1.4
SO_4^{2-}	ND	10

Note: ND = Not detected.

3.10. Defluoridation of field water

The effectiveness of raw DE in fluoride removal from water was tested on a field water (Siloam water) containing 6 mg/L F^- and 3 mg/L PO_4^{3-}. NO_3^- and SO_4^{2-} were not detected. A mixture of the field water and 0.4 g/50 mL of DE with initial pH 2 was equilibrated for 30 min at the shaking of 200 rpm. Centrifuging and fluoride analysis of the supernatant were done following the procedure explained in Subsection 2.3. The concentrations of anions on dilution and after equilibration are reported in Table 5.

The per cent fluoride removal was 14.6%. The reduction of PO_4^{3-} concentration from 2.4 to 1.4 mg/L, representing 41.7% phosphate removal is an indication that phosphate is a high competitor with fluoride in sorption onto DE.

4. Conclusion

The results of defluoridation using raw DE show that the adsorbent is not very effective in removing excess fluoride from water. The maximum per cent fluoride removal and adsorption capacity were 25.62% and 0.6525 mg/g, respectively, for 8 mg/L fluoride spiked water at optimum adsorption conditions (contact time: 30 min, adsorbent dosage: 8 g/L, pH 2, temperature: 298 K and shaking speed: 200 rpm). The sorption data fitted better into Freundlich isotherm which gave linear plots at all evaluated temperatures, thus showing a multi-site adsorption onto the heterogeneous DE surface. The sorption kinetic was observed to be a pseudo-second-order kinetic. Hence, fluoride uptake was by chemisorption. The mechanism controlling the sorption rate was found to be external diffusion of fluoride from the bulk solution to the thin film around the adsorbent particle. Release of metal and non-metal species from DE was observed to be at trace level while there was no detectable release of anions from the adsorbent. Phosphate was observed to have a negative effect on fluoride adsorption at low pH. Modification of DE would be necessary to enhance its fluoride adsorption capacity.

Acknowledgements

References

[1] J.J. Murray (Ed.), Appropriate Use of Fluorides for Human Health, World Health Organization, Geneva, 1986.
[2] M.J. Hammer, Need for fluoridation of desalinated water supplies, Aqua 4 (1986) 179–182.
[3] WHO, Guidelines for Drinking Water Quality, vol. 2 (Health Criteria and other Supporting Information), part III, Chapter 8, World Health Organization, Geneva, 1984.
[4] South African Water Quality Guidelines, Domestic Water Use, second ed., Department of Water Affairs and Forestry, Pretoria, 1996.
[5] A. Abdulrahmani, Fluoride content in drinking water supplies of Riyadh, Saudi Arabia, Environ Monit. Assess. 48 (1996) 261–272.
[6] G.N. Jenkins, The Physiology and Biochemistry of the Mouth, fourth ed., Blackwell Scientific Publication, London, 1978.
[7] E.M. Teri, Endemic Fluorosis: Some Clinical and Epidemiological Aspects of Fluorosis with Specific Reference to Maji ya Chai Area, Arusha Region. A report on domestic water health standards with emphasis on fluoride, Ministry of Water and Energy, Arusha, 1982.
[8] T.A. O'Donnell, The Chemistry of Fluorine, Pergamon Press, Elemsford, NY, 1973.
[9] H. Mjengera, G. Mkongo, Appropriate defluoridation technology for use in fluorotic areas in Tanzania, Phys. Chem. Earth 28 (2003) 1097–1104.
[10] K.W.M. Msonda, W.R.L. Masamba, E. Fabiano, A study of fluoride groundwater occurrence in Nathenje, Lilongwe, Malawi, Phys. Chem. Earth 32 (2007) 1178–1184.
[11] E.J. Ncube, C.F. Schutte, The occurrence of fluoride in South African groundwater: A water quality and health problem, Water SA 31 (2005) 35–40.
[12] T. Rango, A. Vengosh, M. Jeuland, R. Tekle-Haimanot, E. Weinthal, J. Kravchenko, C. Paul, P. McCornick, Fluoride exposure from groundwater as reflected by urinary fluoride and children's dental fluorosis in the main Ethiopian Rift Valley, Sci. Total Environ. 496 (2014) 188–197.
[13] R. Tekle-Haimanot, Z. Melaku, H. Kloos, C. Reimann, W. Fantaye, L. Zerihun, K. Bjorvatn, The geographic distribution of fluoride in surface and groundwater in

Ethiopia with an emphasis on the Rift Valley, Sci. Total Environ. 367 (2006) 182–190.

[14] Z. Amor, M. Taky, S. Malki, S. Nicolas, A. Elmidaoui, Fluoride removal from brackish water by electrodialysis, Desalination 133 (2001) 215–223.

[15] M. Hichour, F. Persin, J. Sandeaux, C. Gavach, Fluoride removal from waters by Donnan dialysis, Sep. Purif. Technol. 18 (2000) 1–11.

[16] C. Venkobachar, L. Iyengar, A.K. Mudgal, Household defluoridation of drinking water using activated alumina, in: Proceedings of the 2nd International Workshop on Fluorosis Prevention and Defluoridation of Water, Nazreth, Ethiopia, November 19–25, 1997.

[17] S. Ghorai, K.K. Pant, Equilibrium, kinetics and breakthrough studies for adsorption of fluoride on activated alumina, Sep. Purif. Technol. 42 (2005) 265–271.

[18] W.M. Gitari, T. Ngulube, V. Masindi, J.R. Gumbo, Defluoridation of groundwater using Fe^{3+}-modified bentonite clay: Optimization of adsorption conditions, Desalin. Water Treat. (2013) 1–13, doi: 10.1080/19443994.2013.855669.

[19] C. Janardhana, G.N. Rao, R.S. Sathish, V.S. Lakshman, Study on defluoridation of drinking water by impregnation of metal ions in activated charcoal, Indian J. Chem. Technol. 13 (2006) 414–416.

[20] M.S. Onyango, T.Y. Leswifi, A. Ochieng, D. Kuchar, F.O. Otieno, H. Matsuda, Breakthrough analysis for water defluoridation using surface-tailored zeolite in a fixed bed column, Ind. Eng. Chem. Res. 48 (2009) 931–937.

[21] S.M. Maliyekkal, S. Shukla, L. Philip, I.M. Nambi, Enhanced fluoride removal from drinking water by magnesia-amended activated alumina granules, Chem. Eng. J. 140 (2008) 183–192.

[22] C.-K. Na, H.-J. Park, Defluoridation from aqueous solution by lanthanum hydroxide, J. Hazard. Mater. 183 (2010) 512–520.

[23] C.S. Sundaram, N. Viswanathan, S. Meenakshi, Defluoridation chemistry of synthetic hydroxyapatite at nano scale: Equilibrium and kinetic studies, J. Hazard. Mater. 155 (2008) 206–215.

[24] P. Yuan, D.Q. Wu, H.P. He, Z.Y. Lin, The hydroxyl species and acid sites on diatomite surface: A combined IR and Raman study, Appl. Surf. Sci. 227 (2004) 30–39.

[25] D.J. Killedar, D.S. Bhatgava, Feasibility of fluoride adsorption on bone charcoal, J. Inst. Eng. 70 (1990) 47–49.

[26] M. Rai, M. Pathan, A. Khan, M. Farooqui, A. Zaheer, A study of the removal of dyes by Goda sand, J. Indian Chem. Soc. 81 (2004) 484–487.

[27] T. Gavriloaiei, D.-I. Gavriloaiei, Determination of surface charge for metal oxides, Analele Stiintifice Universitatii "Al I Cuza" Geologie Tomul LIV (2008) 11–18.

[28] M.A.M. Khraisheh, Y.S. Al-degs, W.A.M. Mcminn, Remediation of wastewater containing heavy metals using raw and modified diatomite, Chem. Eng. J. 99 (2014) 177–184.

[29] R. Yao, F. Meng, L. Zhang, D. Ma, M. Wang, Defluoridation of water using neodymium-modified chitosan, J. Hazard. Mater. 165 (2009) 454–460.

[30] S. Sadiju, C. Kayira, W. Masamba, J. Mwatseteza, Defluoridation of groundwater using bauxite: rural domestic defluoridation technology, Environ. Nat. Resour. Res. 2(3) (2012) 1–9.

[31] N.A. Oladoja, B. Helmreich, Batch defluoridation appraisal of aluminium oxide infused diatomaceous earth, Chem. Eng. J. 258 (2014) 51–61.

[32] D.G. Kinniburgh, General purpose adsorption isotherms, Environ. Sci. Technol. 20 (1986) 895–904.

[33] H.M.F. Freundlich, Over the adsorption in solution, J. Phys. Chem. 57 (1906) 370–485.

[34] K.S. Papageorgiou, K.F. Katsaros, P.E. Kouvelos, W.J. Nolan, H. LeDeit, K.N. Kanellopoulos, Heavy metal sorption by calcium alginate beads from *Laminaria digitata*, J. Hazard. Mater. 137 (2006) 1765–1772.

[35] R. Chang, Physical Chemistry with Applications to Biological Systems, Macmillan Publishing Co. Inc., New York, NY, 1977.

[36] W.J. Weber, F.A. DiGiano, Process Dynamics in Environmental Systems, Environ. Sci. Technol. Series, Wiley and Sons, New York, NY, 1996.

[37] C.H.S. Gulipalli, B. Prasad, K.L. Wasewar, Batch study, equilibrium and kinetics of adsorption of selenium using rice husk ash (RHA), J. Eng. Sci. Technol. 6 (2011) 586–605.

[38] S. Lagergren, Zur theorie der sogenannten adsorption gelöster stoffe (About the theory of so-called adsorption of soluble substances), K. Sven. Vetenskapsakad. Handl. 24 (1898) 1–39.

[39] W.J. Weber, J.C. Morris, Kinetics of adsorption on carbon from solution, J. Sanit. Eng. Div./Am. Soc. Civ. Eng. 89 (1963) 31–60.

[40] C.K. Lee, K.S. Low, S.L. Chew, Removal of anion dyes by water hyacinth roots, Adv. Environ. Res. 3 (1999) 343–351.

[41] M.A.M. Khraisheh, Y.S. Al-Degs, S.J. Allen, M.N. Ahmad, Elucidation of controlling steps of reactive dye adsorption on activated carbon, Ind. Eng. Chem. Res. 41 (2002) 1651–1657.